



## Effect of thiadiazole derivatives on the corrosion of brass in natural seawater by electrochemical techniques

X. Joseph Raj, N. Rajendran

Department of Chemistry, Anna University, Chennai – 600 025, India

Received 13 July 2013, Revised 24 July 2013, Accepted 24 July 2013

Email: [drjosephrajxavier@gmail.com](mailto:drjosephrajxavier@gmail.com) Tel: +91-44-22358659

### Abstract

The inhibiting effect of thiadiazole derivatives namely, 2-Amino-1,3,4-thiadiazole (ATD), 2-Amino-5-methyl-1,3,4-thiadiazole (AMTD) and 2-Amino-5-methylthio-1,3,4-thiadiazole (AMTTD) on 65-35 brass corrosion in natural seawater was studied by potentiodynamic polarization and electrochemical impedance spectroscopy. The results obtained revealed that these compounds were found to be mixed type inhibitors. The magnitude of polarization resistance values and, consequently, the inhibition efficiencies are influenced by the molecular structure of thiadiazole derivatives. Inductively Coupled Plasma Atomic Emission Spectroscopic (ICP-AES) analysis confirmed that dezincification was minimized to a greater extent in the presence of the inhibitors. The adsorption of inhibitors on the brass surface was characterized using Fourier Transform Infrared Spectroscopy (FTIR) and Scanning Electron Microscopy (SEM). The EDX spectra of the brass exposed to inhibitor-containing solutions revealed the presence of the nitrogen and sulphur atoms on the surface.

**Keywords:** Thiadiazole derivatives, Brass, Polarization, Impedance, Adsorption, dezincification

### 1. Introduction

Copper alloys are widely used materials in various heating, cooling systems and other industries due to their high thermal conductivity, good resistance to corrosion and good mechanical workability. Brass has been widely used for shipboard condenser, power plant condenser and petrochemical heat exchanger [1, 2]. Even though copper and copper alloys are corrosion resistant, they are prone to corrosion in oxygen, high concentration of chloride, sulphate, sulphide and nitrate ions containing solutions. Brass is susceptible to corrosion process known as dezincification by means of which brass loses its valuable physical and mechanical properties leading to structural failure and this tendency increases with increasing zinc content of the brass [3]. Many techniques have been used to minimize the dezincification and corrosion of brasses. One of the techniques for minimizing corrosion is the use of inhibitors. The effectiveness of the inhibitor varies with its structure, concentration, the corrosive medium and the surface properties of the alloy. Many inhibitors have been used to minimize the corrosion of brass in different media [4, 5].

It was reported [6-8] that organic compounds containing polar groups including nitrogen, sulfur and oxygen and heterocyclic compounds with polar functional groups and conjugated double bonds inhibited corrosion of brass. Polar functional groups are regarded as the reaction centre that stabilizes the adsorption process. In addition, the adsorption of an inhibitor on a metal surface depends on the nature and the surface charge of the metal, the adsorption mode, its chemical structure and the type of the electrolyte solution [9]. Although there is an extensive literature on the corrosion properties of azole derivatives such as benzimidazole, benzotriazole and tetrazole on steel, copper and its alloys [10,11], there are very few reports devoted to the thiadiazole derivatives on the corrosion and dezincification of brass. Loto et al. discussed in their review the role of thiadiazole derivatives as corrosion inhibitors [12].

In the present work, the electrochemical behavior of 65-35 brass in natural seawater in the absence and presence of thiadiazole derivatives such as 2-Amino-1,3,4-thiadiazole (ATD), 2-Amino-5-methyl-1,3,4-thiadiazole (AMTD) and 2-Amino-5-methylthio-1,3,4-thiadiazole (AMTTD) has been investigated by electrochemical techniques such as polarization and electrochemical impedance spectroscopy. The adsorption of thiadiazole derivatives on brass was carried out using FT-IR spectroscopy. The surface morphological studies were carried out using Scanning Electron Microscope (SEM) and the composition of brass surface was analyzed using energy dispersive X-ray analysis (EDX).

## 2. Experimental

### 2.1. Materials

The chemical composition (wt%) of the brass specimens used was 65.3 % Cu, 34.44 % Zn, 0.1385 % Fe, 0.0635 % Sn and trace amounts of Pb, Mn, Ni, Cr, As, Co, Al and Sr. The electrolyte used was the natural seawater collected in a sterilized brown flask from Eliot beach on the southern coast of Chennai, India (Indian Ocean) containing Cl<sup>-</sup> (20 400 mg L<sup>-1</sup>), Na<sup>+</sup> (11 820 mg L<sup>-1</sup>), Mg<sup>2+</sup> (1010 mg L<sup>-1</sup>), Ca<sup>2+</sup> (394 mg L<sup>-1</sup>), SO<sub>4</sub><sup>2-</sup> (1250 mg L<sup>-1</sup>), and HCO<sub>3</sub><sup>-</sup> (219 mg L<sup>-1</sup>), whereas others species were at lower concentrations [13]. The pH was 8.3. The brass specimens were polished mechanically with different grades of silicon carbide papers (400 - 1200) and were thoroughly washed with double distilled water, then degreased in acetone using ultrasonic vibrator and again thoroughly washed with double distilled water and dried. The thiadiazole derivatives namely, 2-amino-1, 3, 4-thiadiazole (ATD), 2-amino-5-methyl-1, 3, 4-thiadiazole (AMTD) and 2-amino-5-methylthio-1, 3, 4-thiadiazole (AMTTD) and absolute ethanol obtained from Sigma Aldrich were used without further purification. The structures of thiadiazole derivatives are shown in Fig.1.

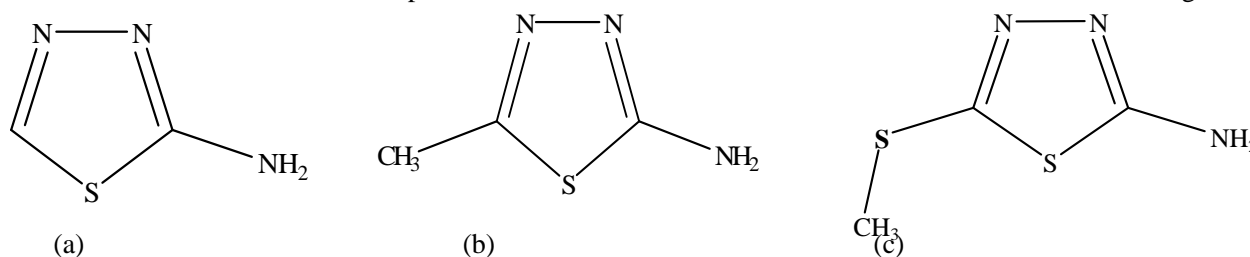


**Fig. 1** Structure of organic inhibitors, (a) 2-Amino-1, 3, 4-thiadiazole, (b) 2-Amino-5-methyl-1, 3, 4-thiadiazole and (c) 2-Amino-5-methylthio-1, 3, 4-thiadiazole

### 2.2 Electrochemical studies

The potentiodynamic polarization studies were carried out with brass specimens having an exposed area of 1 cm<sup>2</sup>. A conventional three electrode cell of volume 300 ml was used for all the electrochemical measurements. The cell assembly consisted of brass as working electrode, a platinum plate as counter electrode and an Ag/AgCl electrode as a reference electrode (Advance-Tech Controls Pvt Ltd, India) in saturated KCl solution with a Luggin capillary bridge. Natural seawater collected from the coastal area of Chennai, India served as the electrolyte. The potentiostat/galvanostat (model PGSTAT 12, AUTOLAB, the Netherlands B.V) controlled by a personal computer with dedicated software (GPES version 4.9.005) was used for conducting the polarization experiments. The cathodic and anodic polarization curves for brass specimen in the test solution were recorded at a sweep rate of 1 mV s<sup>-1</sup> between -600 mV to +200 mV. AC impedance measurements were conducted at room temperature using an AUTOLAB with Frequency response analyzer (FRA), which included a potentiostat model PGSTAT 12. An AC sinusoid of ± 10 mV was applied at the open circuit potential. The frequency range of 100 KHz–50 mHz was employed. Triplicate measurements were made to check the reproducibility of the results.

### 2.3. Inductively Coupled Plasma Atomic Emission Spectroscopy (ICP-AES)

The concentration of copper and Zinc in the electrolytes, after the polarisation experiments in the presence and absence of 10<sup>-3</sup> M piperidine derivatives, were determined by Inductively Coupled Plasma Atomic Emission Spectroscopy (ARCOS from M/s. Spectro, Germany). The dezinification factor ( $z$ ) was calculated using the equation 1 [14],

$$z = \frac{[C_{Zn}/C_{Cu}]_{sol}}{[C_{Zn}/C_{Cu}]_{alloy}} \quad (1)$$

where,  $[C_{Zn}/C_{Cu}]_{sol}$  and  $[C_{Zn}/C_{Cu}]_{alloy}$  are the ratios between the concentrations of zinc and copper in the solution and in the alloy respectively.

### 2.4. Surface morphology

The brass surface was prepared by keeping the specimens for an hour in the electrolyte with and without the optimum concentrations of the inhibitors. The brass specimens were then washed with distilled water, dried and analyzed using SEM/EDX. A Philips model XL30SFEG scanning electron microscope with an energy dispersive X-ray analyzer attached was used for surface analysis. The film that has developed on the brass surface in the presence of the inhibitor was washed with water, dried and collected by scrapping from the surface of the alloy for subsequent spectral anal Fourier Transform Infrared Spectroscopy (FTIR) analysis. Infrared spectra were obtained from KBr discs using a Perkin-Elmer Model 577 spectrometer.

### 3. Results and discussion

#### 3.1. Electrochemical measurements

The potentiodynamic anodic and cathodic polarization curves of brass in natural seawater in the presence and absence of different concentrations of ATD, AMTD and AMTTD are shown in the Fig. 2.

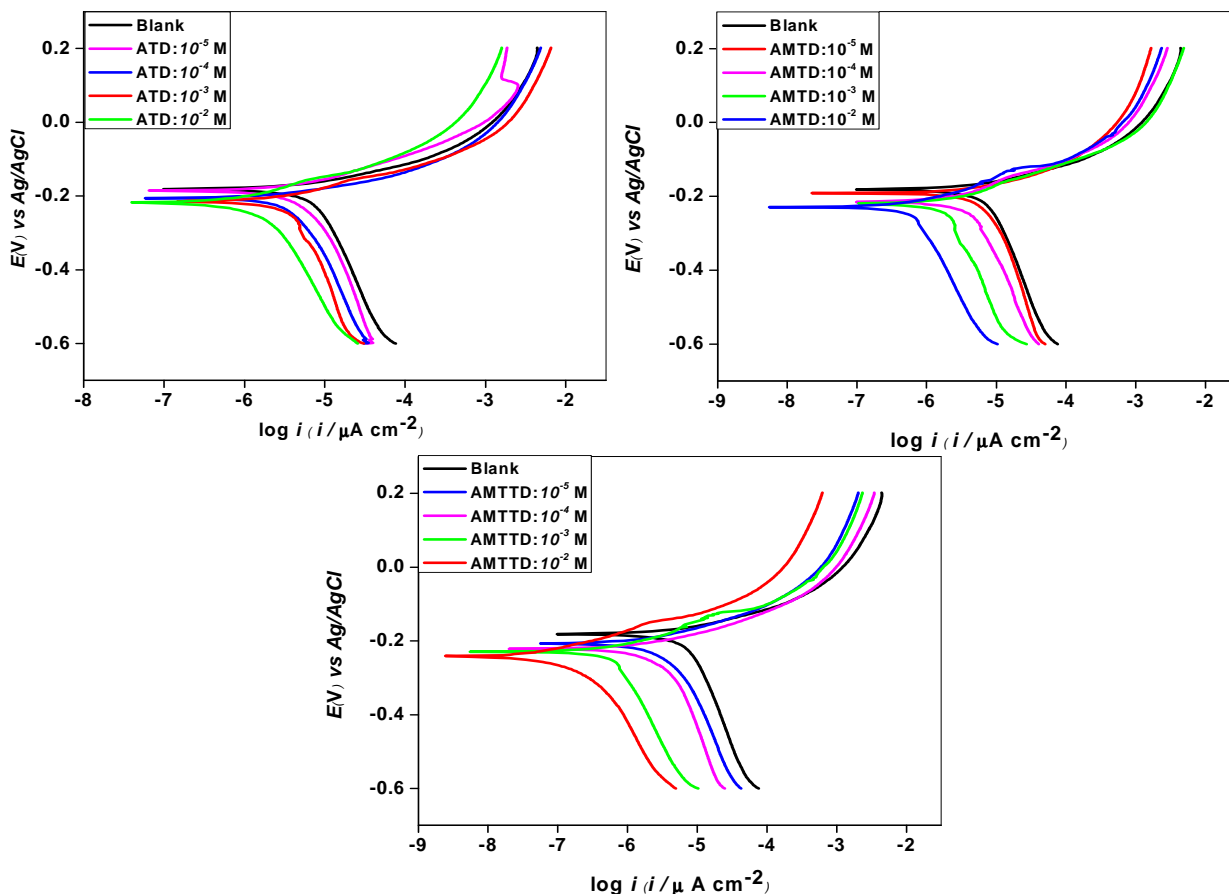


**Fig. 2** Polarisation curves for brass in seawater containing different concentrations of ATD, AMTD and AMTTD

It is evident that in the presence of thiazazole derivatives, the cathodic and anodic polarization curves were shifted to negative potential region and the shift was found to increase with increasing inhibitor concentration. This observation clearly indicated that the inhibitors control both cathodic and anodic reactions and thus act as mixed-type inhibitors. The polarization parameters such as corrosion potential ( $E_{\text{corr}}$ ) and corrosion current ( $I_{\text{corr}}$ ) were obtained by extrapolation of the Tafel lines. The  $E_{\text{corr}}$  values were shifted slightly in the presence of thiazazole derivatives. The corrosion current ( $I_{\text{corr}}$ ) decreased with increasing concentration of inhibitor. The inhibition efficiency (IE) was calculated using the equation 2 [15] and the values are presented in Table 1.

$$IE (\%) = \frac{I_{\text{corr}} - I_{\text{corr(inh)}}}{I_{\text{corr}}} \times 100 \quad (2)$$

where,  $I_{\text{corr}}$  and  $I_{\text{corr(inh)}}$  are the corrosion current density values without and with inhibitors, respectively. It can be shown from the table that with increasing inhibitor concentration, corrosion current density ( $I_{\text{corr}}$ ) decreases and inhibition efficiency (IE) increases. For instance,  $I_{\text{corr}}$  of brass in the absence and in the presence of  $10^{-2}$  M of ATD, AMTD and AMTTD was  $2.61 \mu\text{A cm}^{-2}$ ,  $0.61 \mu\text{A cm}^{-2}$ ,  $0.38 \mu\text{A cm}^{-2}$  and  $0.28 \mu\text{A cm}^{-2}$ , respectively. The best inhibition efficiency observed was 89 % for AMTTD at  $10^{-2}$  M concentration and 85 % for AMTD and 77 % for ATD at the same concentration. The values of cathodic Tafel slope  $\beta_c$  and anodic Tafel slope  $\beta_a$  are found to change with increasing inhibitor concentration indicating that the inhibitors control both anodic and cathodic reactions. It was confirmed that with increase in inhibitor concentration corrosion rate decreases. The corrosion inhibition efficiency of these compounds increases in the order, ATD < AMTD < AMTTD. Highest IE of AMTTD is due to the presence of additional S atom with lone pair of  $\pi$  electrons. These electrons interact with the vacant d-orbital of copper present in the brass surface and adsorb strongly. The better

efficiency of AMTD compared to ATD is due to the presence of electron donating methyl group in its structure. It can be seen that the structure of the side chain also has a significant effect on the inhibition efficiencies. The values of inhibition efficiency increase with increase in inhibitor concentration, indicating that a higher surface coverage was obtained in a solution with maximum inhibitor concentration.

**Table 1** Tafel polarization parameters for the corrosion of brass in natural seawater in the presence and absence of different concentrations of ATD, AMTD and AMTTD

Compound	Concn (M)	E <sub>corr</sub> (mV)	I <sub>corr</sub> (μA cm <sup>-2</sup> )	β <sub>c</sub> mV/dec	β <sub>a</sub> mV/dec	R <sub>p</sub> (Ω)	CR (mmpy) x 10 <sup>-3</sup>	IE (%)
Blank	-	-180	2.61	45	65	522	110	-
ATD	10 <sup>-5</sup>	-185	1.84	61	83	737	77	30
	10 <sup>-4</sup>	-207	1.21	69	86	824	50	54
	10 <sup>-3</sup>	-214	0.73	78	91	1405	30	73
	10 <sup>-2</sup>	-219	0.61	85	104	2060	25	77
	10 <sup>-5</sup>	-192	1.81	63	84	780	75	31
AMTD	10 <sup>-4</sup>	-214	1.09	79	97	1410	46	58
	10 <sup>-3</sup>	-221	0.46	85	98	2170	20	82
	10 <sup>-2</sup>	-229	0.38	99	118	4060	16	85
	10 <sup>-5</sup>	-206	1.74	72	89	810	73	33
AMTTD	10 <sup>-4</sup>	-221	0.57	84	96	2145	24	78
	10 <sup>-3</sup>	-229	0.35	98	114	4260	14	87
	10 <sup>-2</sup>	-241	0.28	117	139	5180	12	89

The Nyquist impedance plots obtained for the brass electrode at an open-circuit potential after one hour immersion in seawater in the absence and presence of different concentrations of ATD, AMTD and AMTTD are shown in the Fig. 3. The quantitative analysis of these spectra was performed using the equivalent circuit shown in Figs 4a and 4b. The equivalent circuit obtained is similar to the reported circuit for the corrosion mechanism in chloride media [16]. These Nyquist impedance plots have different shapes at different concentrations showing that there is a change in the corrosion mechanism due to the addition of inhibitors. It was found that the results obtained in the absence of thiadiazole derivatives can be represented by two capacitive loops. The equivalent circuit model  $R_s [C_{dl} R_{ct} (C_F R_F)]$  is used for fitting the impedance data for the blank solution. On the other hand, the equivalent circuit model  $R_s \{ C_f R_f (C_{dl} R_{ct}) [ C_F R_F ] \}$  is used for fitting the impedance data in the presence of inhibitors. The calculated parameters obtained from equivalent circuit fitting analysis with and without inhibitor in seawater are given in Table 2.

It can be seen from the table that with increase in inhibitor concentration,  $R_{ct}$  value increased from 2.7 kΩ cm<sup>2</sup> for the blank solution to 11.3 kΩ cm<sup>2</sup> for ATD, 17.9 kΩ cm<sup>2</sup> for AMTD and 31.2 kΩ cm<sup>2</sup> for AMTTD, whereas  $C_{dl}$  value decreased from 173 μF cm<sup>2</sup> for the blank solution to 27 μF cm<sup>2</sup> for ATD, 22 μF cm<sup>2</sup> for AMTD and 10 μF cm<sup>2</sup> for AMTTD. The decrease in  $C_{dl}$  value is due to the decrease in local dielectric constant and/or an increase in the thickness of the electrical double layer, suggests that the thiadiazole derivatives function by adsorption at the metal-solution interface. The decrease in  $C_{dl}$  value upon increase in inhibitor concentration was due to reduced access of charged species to the brass surface, as inhibitor has adsorbed and a good persistent layer of the same was formed on the brass surface. The change in  $R_{ct}$  and  $C_{dl}$  values was caused by the gradual replacement of water molecules by the anions of the NaCl present in seawater and adsorption of the organic inhibitor molecules on the metal surface, reducing the extent of dissolution.

The value of Faradic resistance ( $R_F$ ) increases with increase in concentration showing that ATD, AMTD and AMTTD stabilize the corrosion products on the metal surface and the value reaches more than 12 times greater value for AMTTD than that obtained for the blank solution. Faradic resistance value reaches a maximum of 13.4 kΩ cm<sup>2</sup>, 21.1 kΩ cm<sup>2</sup> and 35.2 kΩ cm<sup>2</sup> for ATD, AMTD and AMTTD at 10<sup>-2</sup> M concentration respectively. As the concentration of the inhibitor increases, the inhibitors get adsorbed effectively on the brass surface which increases the  $R_{ct}$  values and decreases the  $C_F$  values. The value of faradic capacitance is maximum for the blank solution and is equal to 30 μF cm<sup>2</sup> and the values for 10<sup>-2</sup> M concentration of ATD, AMTD and AMTTD decreased to 11 μF cm<sup>2</sup>, 9 μF cm<sup>2</sup> and 7 μF cm<sup>2</sup> respectively. It is also observed from the table that  $n_F$  values increases with increase in concentrations and are significantly greater than 0.5.

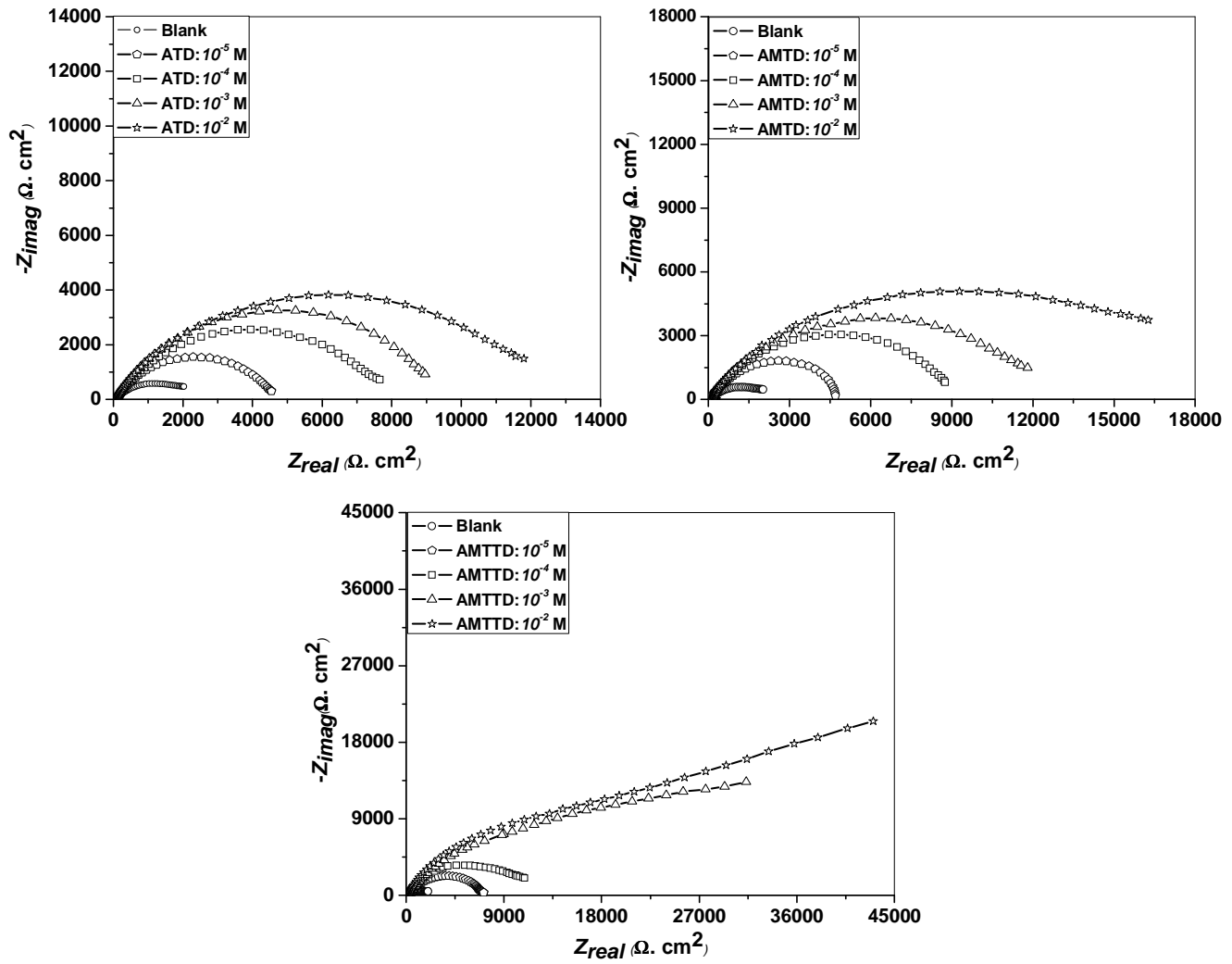


**Fig. 3** Nyquist plot for brass in seawater containing different concentrations of ATD, AMTD and AMTTD

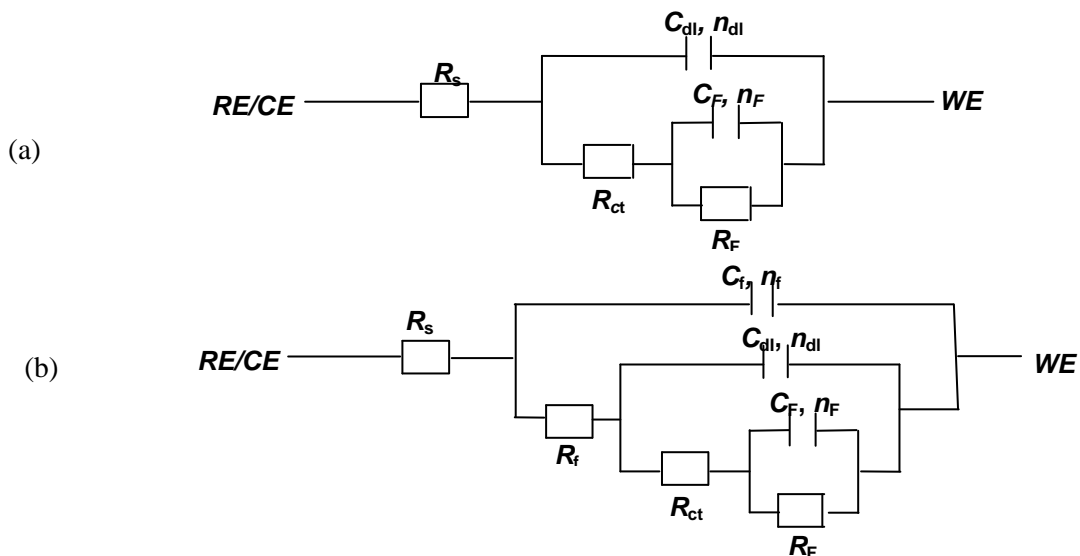


**Fig. 4** Computer fitted equivalent electrical circuits of the experimental impedance data (a)  $R_s [C_{dl} R_{ct} (C_F R_F)]$  and (b)  $R_s \{ C_f R_f (C_{dl} R_{ct}) [ C_F R_F] \}$

Inhibition efficiency (IE) increased with increase in inhibitor concentrations and this corresponds with increase in  $R_p$  values indicating that better inhibition efficiency was obtained due to better adsorption of inhibitor molecules on the brass surface. The inhibition efficiency reaches a maximum of 78 for ATD, 86 for AMTD and

91 for AMTTD at  $10^{-2}$  M. As the concentration of the inhibitor increases,  $R_f$ ,  $R_{ct}$  and  $R_F$  values increases steeply whereas the capacitive values decreases. Due to the difference in their molecular structures, thiazazole derivatives viz., ATD, AMTD and AMTTD show differences in their inhibition efficiency.

**Table 2** Electrochemical parameters for corrosion of brass in natural seawater in the presence and absence of different concentration of ATD, AMTD and AMTTD

Inhibitor conc. (M)	$R_s$ ( $\Omega$ $cm^2$ )	$R_f$ ( $k\Omega$ $cm^2$ )	$C_f$ ( $\mu F$ $cm^2$ )	$n_f$	$R_{ct}$ ( $k\Omega$ $cm^2$ )	$C_{dl}$ ( $\mu F$ $cm^2$ )	$n_{dl}$	$R_F$ ( $k\Omega$ $cm^2$ )	$C_F$ ( $\mu F$ $cm^2$ )	$n_F$	IE (%)
Blank	45	-	-	-	2.7	173	0.5	3.2	30	0.6	-
ATD											
$10^{-5}$	60	0.6	74	0.6	3.5	113	0.6	4.3	16	0.6	31
$10^{-4}$	67	0.9	68	0.7	5.6	72	0.6	6.3	14	0.7	55
$10^{-3}$	75	1.2	33	0.7	9.6	37	0.7	11.1	13	0.7	73
$10^{-2}$	102	1.3	29	0.8	11.3	27	0.7	13.4	11	0.8	78
AMTD											
$10^{-5}$	69	1.0	62	0.7	3.4	111	0.6	4.2	15	0.6	32
$10^{-4}$	95	1.2	45	0.7	6.1	63	0.7	7.6	13	0.7	59
$10^{-3}$	102	1.3	27	0.8	13.6	26	0.7	15.6	10	0.8	81
$10^{-2}$	173	1.5	13	0.8	17.9	22	0.7	21.1	9	0.8	86
AMTTD											
$10^{-5}$	146	1.2	44	0.8	3.5	98	0.7	4.3	14	0.6	34
$10^{-4}$	228	1.3	28	0.8	11.2	60	0.7	13.6	13	0.7	78
$10^{-3}$	243	1.6	12	0.9	21.4	20	0.7	25.1	9	0.8	88
$10^{-2}$	272	1.7	9	0.9	31.2	10	0.8	35.2	7	0.9	91

\*  $R_{p(inh)} = R_f + R_{ct} + R_F$  and  $R_p = R_{ct} + R_F$ ;  $R_s$  – Electrolyte resistance,  $R_{ct}$  – Charge-transfer resistance,  $C_{dl}$  – Charge-transfer capacitance,  $R_F$  – Faradic resistance,  $C_F$  – Faradic capacitance,  $R_f$  – Film resistance,  $C_f$  – Capacitance due to surface film and  $n_f$ ,  $n_{dl}$  &  $n_F$  – Coefficients representing the depressed characteristic of the three capacitive loops.

### 3.2. Adsorption Isotherm

The degree of surface coverage,  $\theta$  at different inhibitor concentrations of ATD, AMTD and AMTTD in natural seawater was evaluated to explain the best isotherm to determine the adsorption process. The linear relationship between  $\theta$  values and  $C_{inh}$  are to be found in order to obtain the isotherm. Attempts were made to fit the  $\theta$  values to various isotherms including Langmuir, Temkin, Frumkin and Flory-Huggins. The best fit is obtained with the Langmuir isotherm. The Langmuir adsorption isotherm is given by the equation 3[17]:

$$\frac{C_{inh}}{\theta} = C_{inh} \pm \frac{1}{K} \quad (3)$$

where,  $C_{inh}$  is the concentration of inhibitor,  $\theta$  is the fractional surface coverage and  $K$  is the adsorption equilibrium constant. A plot of  $C_{inh}/\theta$  against  $C_{inh}$  shows a straight line indicating that adsorption follows the Langmuir adsorption isotherm as shown in Fig. 5. The equilibrium constant of adsorption  $K_{ads}$  is related to the free energy of adsorption ( $\Delta G_{ads}$ ) by the equation 4:

$$\Delta G_{ads} = -2.303RT \log (55.5 K) \quad (4)$$

where,  $R$  is the universal gas constant,  $T$  is the absolute temperature and the molar concentration of water per litre is 55.5. The values of  $K_{ads}$  are 2703, 4556 and 6692  $dm^3 \cdot mol^{-1}$  respectively and that of  $\Delta G_{ads}$  are -30.03, -31.35 and -32.32 kJ/mol for ATD, AMTD and AMTTD respectively. The negative values of  $\Delta G_{ads}$  show the spontaneity of the adsorption process and stability of the adsorbed layer on the brass surface [18]. The values of  $\Delta G_{ads}$  in our measurements was more than -20 kJ/mol, suggesting that ATD, AMTD and AMTTD at  $10^{-3}$  M chemisorbed on the brass surface.

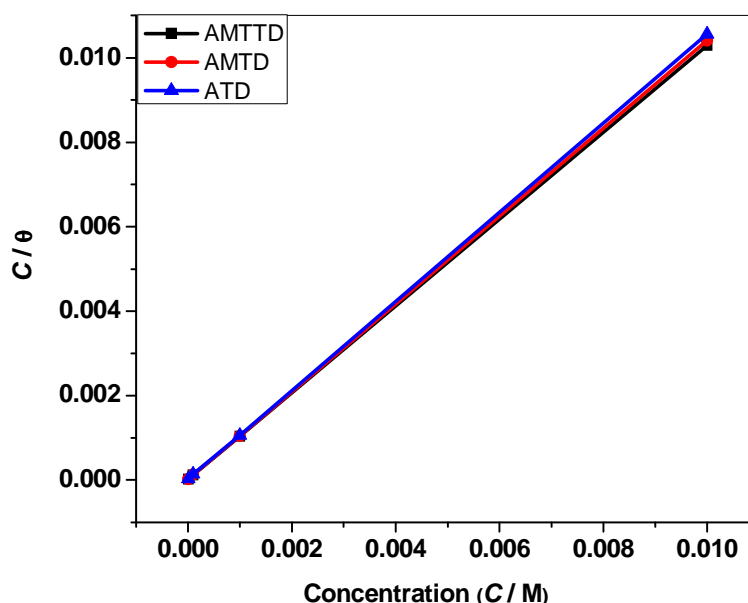


Fig. 5 Adsorption isotherm of brass in seawater containing various concentrations of ATD, AMTD and AMTTD

### 3.3. FTIR Analysis

The FTIR analysis of ATD, AMTD and AMTTD and their brass complexes was carried out between  $500\text{ cm}^{-1}$  and  $4000\text{ cm}^{-1}$ . The spectrum is shown in Fig. 6.

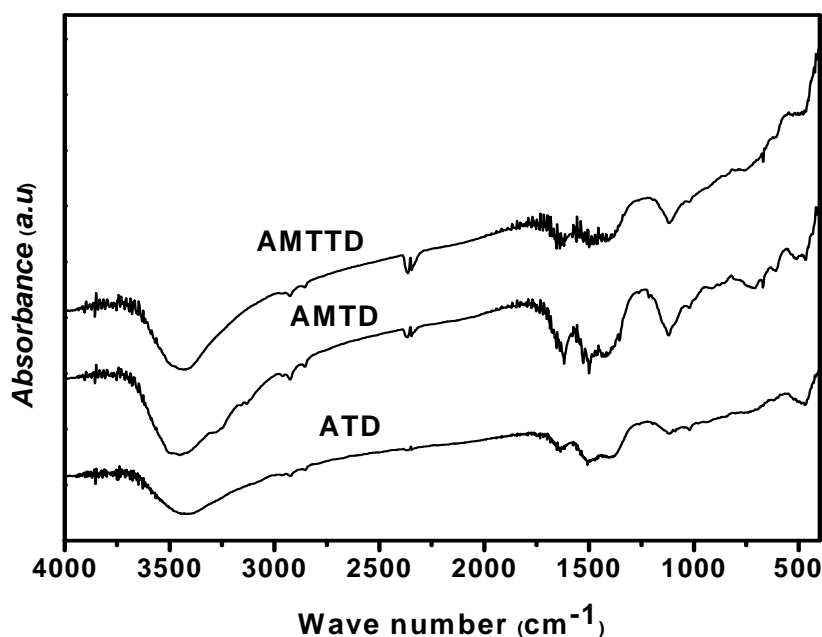


Fig. 6 FTIR spectra of the inhibitor film formed on brass surface

The infrared absorption bands become very useful for determining the mode of coordination of the ligand to metal. The IR spectra of the compounds show two bands due to the  $\text{-NH}_2$  group at around  $3285\text{--}3262\text{ cm}^{-1}$  and  $3111\text{--}3091\text{ cm}^{-1}$ , whereas in the metal complexes the band is shifted and show a single band in the region around  $3454\text{--}3428\text{ cm}^{-1}$ , which indicates the involvement of the ligand in complexation after deprotonation. The strong bands observed at around  $1640\text{--}1619\text{ cm}^{-1}$  range in the free ligand have been assigned to  $\nu(\text{C}=\text{N})$  stretching vibrations. On complexation, these bands were observed to be shifted to lower frequencies between  $1628\text{--}1612\text{ cm}^{-1}$ . The negative shift of these bands in the complexes indicates the coordination of ring nitrogen atoms of the thiadiazole derivatives. For the three compounds the N–N stretching of the thiadiazole ring is observed in the

range around 1529 and 1510  $\text{cm}^{-1}$ . After complexation the values are shifted to lower region between 1500 and 1490  $\text{cm}^{-1}$  due to the restriction of vibration of the ring atoms. The peaks at 1137 and 1197  $\text{cm}^{-1}$  respectively for the ATD and AMTD are assigned to C–S stretching of the sulphur atom of the thiadiazole ring. After complexation of the compounds with metal, the peaks were shifted to lower frequencies at 1116 and 1120  $\text{cm}^{-1}$  respectively indicating the involvement of the ring S atom in complexation. The compound AMTTD showed a peak at 1033  $\text{cm}^{-1}$  due to the C–S stretching of the  $\text{CH}_3\text{S}$  group attached to the thiadiazole ring. On complexation of this sulphur atom to the metal, the C–S stretching is shifted to 1119  $\text{cm}^{-1}$ . Thus, the FTIR spectroscopic study reveals that the sulphur and nitrogen atoms present in thiadiazole derivatives form complexes with copper in the brass and forms a film over its surface.

### 3.4. Inductively Coupled Plasma Atomic Emission Spectroscopic (ICP-AES) Analysis

The dezincification (z) factors for brass in the absence and presence of  $10^{-3}$  M of ATD, AMTD and AMTTD in natural seawater were calculated from the ICP-AES data and the results are given in Table 3. The results showed that both copper and zinc were present in the electrolyte in very small quantities and the copper to zinc ratio was found to be lesser than that of the bulk alloy. This is due to the formation of surface film of inhibitor on the metal surface as well as the corrosion product like oxides of copper and zinc as well as polymeric complexes with inhibitors. It is clear from the table that dezincification was much higher in the absence of inhibitors, while dezincification was much lower in the presence of  $10^{-3}$  M concentration of ATD, AMTD and AMTTD. This indicated that the studied inhibitors were able to minimize the dissolution of both zinc and copper.

**Table 3** Effect of ATD, AMTD and AMTTD on the dezincification of brass in natural seawater at optimum concentration ( $10^{-3}$  M) for all inhibitors

Inhibitors	Solution analysis		Dezincification factor (z)	Percent inhibition	
	Cu/ $10^{-8}$ M	Zn/ $10^{-8}$ M		Cu	Zn
	Blank	74		1725	43
ATD	13	198	31	82	88
AMTD	11	169	29	85	90
AMTTD	8	106	25	89	93

### 3.5. SEM and EDX analysis

The SEM micrograph of the brass sample in the absence and presence of optimum concentration of the studied thiadiazole derivatives are shown in Fig. 7. The brass surface in the absence of inhibitors is covered with a layer of corrosion products (Fig. 7a). This is due to the attack of brass surface with aggressive chloride ions in natural seawater. The brass surface is not affected by corrosion in the presence of  $10^{-3}$  M of ATD, AMTD and AMTTD inhibitor molecules. This is due to the formation of copper and zinc complexes of the inhibitors that protect the brass surface against corrosion. The formation of complex with inhibitor is visible in the presence of studied inhibitors and the micrographs are shown in Fig. 7 (b-d). At the optimum concentration of the inhibitors, the surface is covered by a thin layer of inhibitor which effectively controls the dissolution of brass. The complex formed with inhibitors on the brass surface has higher stability and low permeability which provides some corrosion protection to the metal by restricting the mass transfer of reactants and products between the bulk solution and the metal surface.

The presence of the nitrogen and sulphur atoms in the EDX spectra of the brass surface corresponding to the sample containing the optimum concentrations of ATD, AMTD and AMTTD was determined by EDX spectra. Fig. 8 (a-d) presents the EDX spectra for the samples in the absence and presence of optimal concentrations of studied thiadiazole derivatives. In the absence of inhibitor molecules, the EDX spectra confirm the existence of chlorine and oxygen along with copper and zinc due to the formation of  $\text{Cu}_2\text{O}$  and  $\text{CuCl}_2^-$  complex, which shows the passive film contained only by  $\text{Cu}_2\text{O}$  and  $\text{CuCl}_2^-$ . However, in the presence of the optimum concentrations of the ATD, AMTD and AMTTD inhibitors, nitrogen and sulphur atoms are found to be present and coordinated with the brass surface, thus forming the complexes of the studied inhibitors on the brass surface. This indicates that the studied inhibitor molecules are adsorbed on the brass surface, thus protecting the brass surface against corrosion.

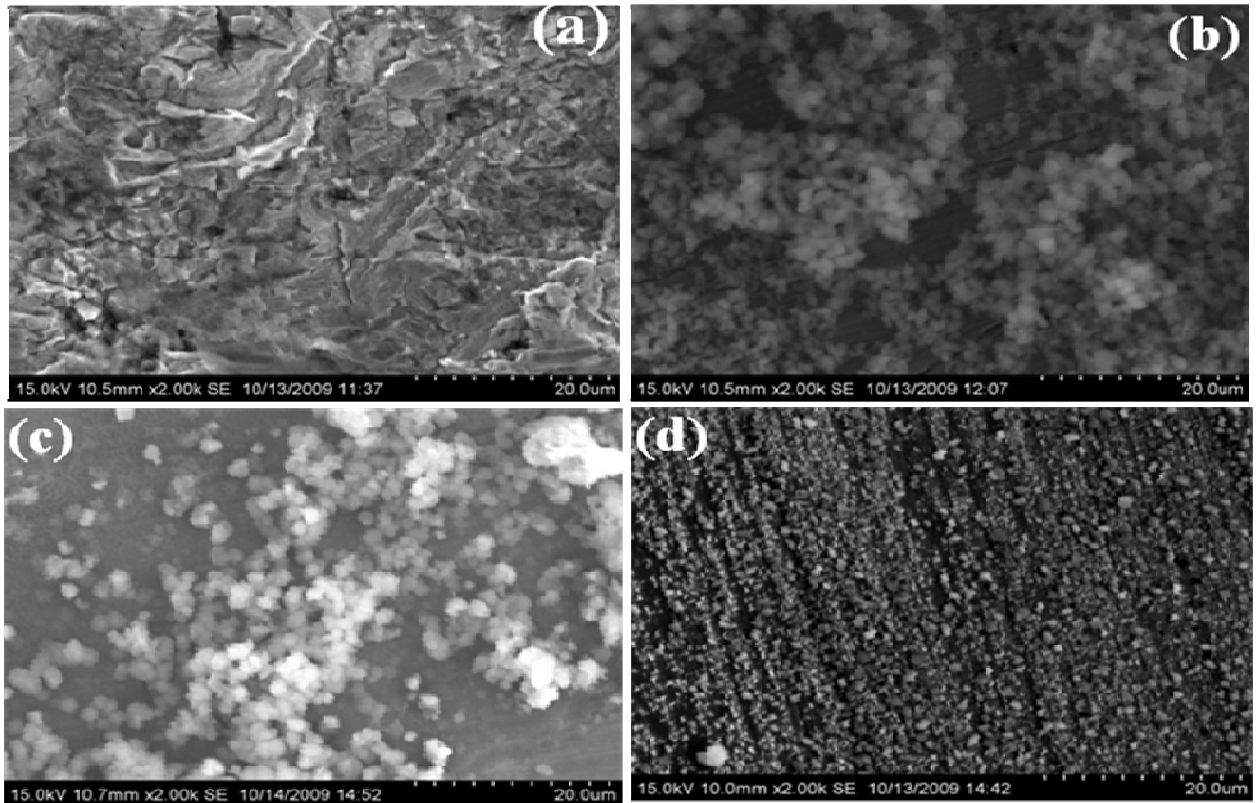


Fig. 7 SEM images for brass surface (a) blank, (b) ATD, (c) AMTD and (d) AMTTD

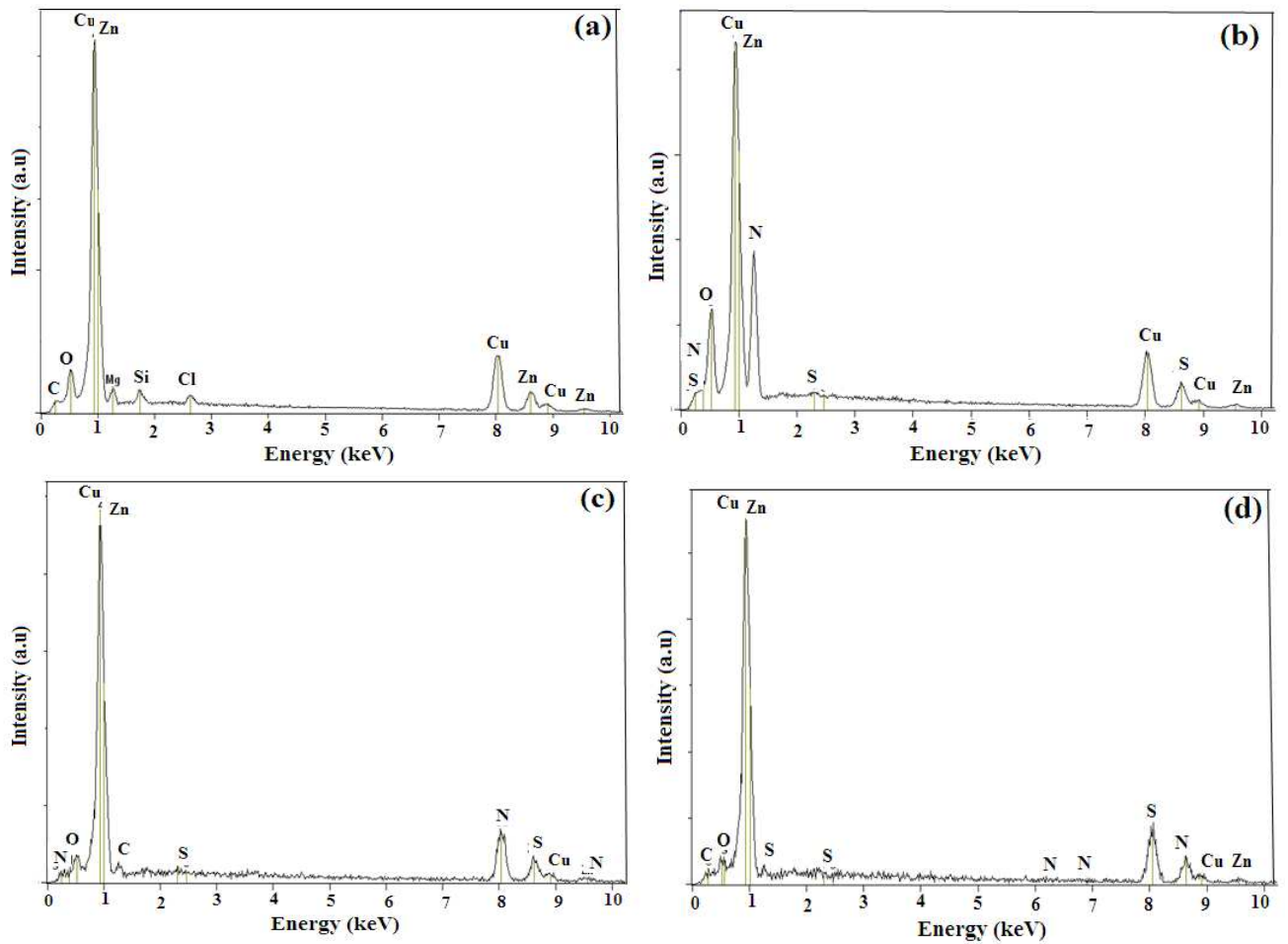


Fig. 8 EDX profile for brass surface (a) blank, (b) ATD, (c) AMTD and (d) AMTTD

### 3.6. Mechanism of corrosion Inhibition

The inhibitor molecules are adsorbed onto the metal surface through electron transfer from the adsorbed species to the vacant *d* orbital in the metal to form a co-ordinate bond with the organic compounds containing nitrogen, sulphur and oxygen. The studied compounds contain two iminic group (-C=N) and one C-S group of thiadiazole ring besides the 2-amino group in ATD, 2-amino-5-methyl group in AMTD and 2-amino-5-methylthio group in AMTTD respectively. The unshared electron pairs on N and S are capable of forming a co-ordination bond with copper which enhances the adsorption of the compounds on the metal surface. It is known that the adsorption of these thiadiazole derivatives on the brass surface occurs directly on the basis of donor behavior of the hetero atoms containing the lone pair of electrons and the extensively delocalized  $\pi$ -electrons of the inhibitor molecules with the acceptor behavior of the vacant *d*-orbitals of brass surface atoms. The AMTTD was found to give excellent inhibition due to the presence of additional electron donating group (-SCH<sub>3</sub>) on the thiadiazole derivative which increases the electron density. This leads to the strong electrostatic attraction of AMTTD on the metal surface thereby resulting in the high inhibition efficiency. The better inhibition performance of AMTD is due to the presence of electron donating methyl group in their structures which increase the electron density of the aromatic ring and makes the  $\pi$ -electrons more available to interact with brass surface. Thus, AMTTD, AMTD and ATD are more effectively adsorbed on the brass surface.

### Conclusion

ATD, AMTD and AMTTD molecules have been investigated as corrosion inhibitors for brass in natural seawater. The substituted thiadiazole derivatives were found to be effective inhibitors for brass corrosion in natural seawater. The polarization data indicate suppression of both the partial corrosion processes in the presence of thiadiazole derivatives. These inhibitors behave as mixed-type. Electrochemical impedance spectroscopy shows that  $R_{ct}$  values increase, while  $C_{dl}$  values decrease in the presence of thiadiazole derivatives. ICP-AES analysis confirmed that dezincification was minimized to a greater extent in the presence of the inhibitors. SEM and EDX investigations indicate that the dissolution of brass decreases due to the strong adsorption of thiadiazole derivatives on the brass surface.

### References

1. Fontana M.G., *Corrosion Engineering*, 3rd ed., McGraw-Hill, New York, 1986, p 86
2. Kear G., Barker B.D., Walsh, F.C. *J. Appl. Electrochem.* 34 (2004) 659.
3. Varvara S., Muresan L.M., Rahmouni K. *Corros. Sci.* 50 (2008) 2596.
4. Sherif E.M., Park S.M. *Electrochim. Acta.* 51 (2006) 6556.
5. Bouklah M., Hammouti B., Aouniti A., Benhadada, T. 49 (2004) 225.
6. Ravichandran R., Rajendran N. *Appl. Surf. Sci.* 241 (2005) 449.
7. Ravichandran R., Rajendran N. *Appl. Surf. Sci.* 239 (2005) 182.
8. Gerengi H., Darowicki., Bereket, G. *Corros. Sci.* 51 (2009) 2573.
9. Sheriff E.M., Park S.M. *Corros. Sci.* 48 (2006) 4065.
10. Bouklah M., Attayibat A., Hammouti B., Ramdani A., Radi S., Benkaddour M. *Appl. Surf. Sci.* 240 (2005) 341.
11. Joseph Raj X., Rajendran N. *J. Solid. State. Electrochem.* 16 (2012) 391.
12. Loto R.T., Loto C.A., Popoola A.P.I., *J. Mater. Environ. Sci.* 3 (5) (2012) 885.
13. Joseph Raj X., Rajendran N. *Int. J. Electrochem.Sci.* 6 (2011) 348.
14. Ravichandran R., Rajendran N. *Appl. Surf. Sci.* 236 (2004) 241.
15. Joseph Raj X., Rajendran N. *Ind. Eng. Chem. Res.* 51 (2012) 30.
16. Curkovic H.O., Stupnisek-Lisac E., Takenouti H. *Corros. Sci.* 52 (2010) 398.
17. Lebrini M., Bentiss F., Vezin H. *Corros. Sci.* 48 (2006) 1279.
18. Al-Nami Samar Y., *J. Mater. Environ. Sci.* 4 (2013) 39

(2014); <http://www.jmaterenvirosnci.com>